Dielectronic-recombination-rate coefficients for neonlike ions

Sam Dalhed, Joseph Nilsen, and Peter Hagelstein
Lawrence Livermore National Laboratory, University of California, Livermore, California 94550
(Received 22 April 1985)

This paper presents for the first time an explicit calculation of the partial dielectronic-recombination-rate coefficients via the $3l3l'$ manifold for 17 neonlike ions ranging from argon to tungsten, using relativistic multiconfiguration wave functions to calculate both the Auger and radiative matrix elements. The effect of electron collisions on the dielectronic-recombination-rate coefficient is also examined at several densities of interest for modeling laboratory plasmas.

I. INTRODUCTION

Dielectronic recombination is the dominant recombination process for ions in high-temperature, low-density plasmas[1] such as the solar corona. It is also a significant contributor to plasma cooling in hot plasmas found in laboratory fusion plasma experiments.[2] The calculation of the dielectronic-recombination-rate coefficient α^{DR} is difficult because of the many intermediate resonance states over which the rate needs to be summed. We calculate α^{DR} for recombination from the neonlike ground state into the sodiumlike nonautoionizing states via the $3l3l'$ manifold for 17 neonlike ions ranging from Ar^{+8} to W^{+64}. This calculation uses accurate relativistic atomic wave functions calculated for each ion. This is the first calculation in which relativistic multiconfiguration wave functions are used to calculate the matrix elements explicitly for each of the doubly excited states. Previous authors have calculated α^{DR} using a simple angular momentum averaged procedure[3] to average over as many intermediate states as possible or have done a detailed calculation using single- or few-configuration nonrelativistic wave functions to calculate the relevant atomic data.[4-6]

II. METHOD

In j-j coupling the $3l3l'$ manifold consists of 237 doubly excited states which are connected to the neonlike ground state $1s^22s^22p^6$ by the Auger process and to the five sodiumlike nonautoionizing states $[KL]3s_{1/2},3p_{1/2},3p_{3/2},3d_{3/2},3d_{5/2}$ by radiative decay and electron collisional deexcitation. In addition, the doubly excited states are connected to each other by radiative decay and electron collisional processes.

There are a total of 243 states in our model. Our first task was to calculate the wave functions for each of these states using the code YODA, which we ran on a Control Data Corporation CDC7600 computer. YODA is a relativistic multiconfiguration Hartree-Fock atomic physics code which uses as its orbital basis a set of single-configuration Dirac orbitals calculated in a spherically symmetric central potential which includes a finite nuclear potential. Racah algebra is used in calculating the angular momentum part of the matrix elements. Using these fixed orbitals to construct the single-configuration wave functions, the Hamiltonian matrix is calculated including Breit corrections to the Coulomb interactions between the electrons. Also included are the quantum electrodynamic effects such as self-energy[7] and vacuum polarization.[8] The Hamiltonian is diagonalized to give the full multiconfiguration wave functions in intermediate coupling. These wave functions are then used to calculate the oscillator strengths for all the dipole-allowed transitions.

The continuum orbitals used in computing the Auger matrix elements were calculated in a distorted wave approximation neglecting exchange. The potential was a spherically averaged final-state potential. For this work, an ion in a neonlike ground state would be used to calculate the potential. For the high-Z systems we are using, the neglect of the exchange term should be a small effect. The free-electron wave functions are used with the multiconfiguration wave functions for the bound electrons to calculate the Auger matrix elements.

Approximate collision cross sections are computed in the classical path approximation[9] coupling dipole-allowed states. These collision cross sections are then approximated by the five-parameter fit

$$\langle \sigma v \rangle = 1.58\times 10^{-5} p(b) \frac{e^{-b}}{b\theta^{3/2}} \text{ cm}^3/\text{sec} , \tag{1}$$

where

$$b = \frac{\delta E}{\theta} \tag{2}$$

and

$$\ln p(b) = a_0 + a_1 \ln b + a_2 \ln^2 b + a_3 \ln^3 b . \tag{3}$$

δE is the transition energy (in eV) used in fitting the data and $\theta = kT$ is the electron temperature (in eV). The free electrons of density n_e are assumed to have a Maxwell-Boltzmann velocity distribution represented by a temperature T.

The components of the dielectronic-recombination process are dielectronic capture, Auger,

$$X^{+z} + e^- \rightarrow X^{+(z-1)}(\overline{2l}_1 3l_2 3l_3) ,$$

and stabilization,

$$X^{+(z-1)}(\overline{2l}_1 3l_2 3l_3) \rightarrow X^{+(z-1)}(3l_3) + h\nu .$$

The neonlike ground state X^{+z} captures an electron to form a doubly excited sodiumlike state $X^{+(z-1)}(\bar{2}l3l3l')$. The notation $\bar{2}l$ represents a hole in the neonlike core, while $3l3l'$ represents the two $n=3$ electrons. The doubly excited state can Auger decay or undergo a radiative decay ($\Delta n=1$) to a sodiumlike nonautoionizing state which stabilizes the capture process.

In addition to the "direct" dielectronic recombination there are radiative processes and (for finite density plasmas) collisional processes which can cause angular momentum redistribution within the doubly excited states and collisional deexcitation to the sodiumlike nonautoionizing states which stabilize the capture. These processes are the following: radiative decay processes,

$$X^{+(z-1)}(\bar{2}l_1 3l_2 3l_3)\rightarrow X^{+(z-1)}(\bar{2}l_1 3l_2' 3l_3)+h\nu ,$$

$$X^{+(z-1)}(\bar{2}l_1 3l_2 3l_3)\rightarrow X^{+(z-1)}(\bar{2}l_1' 3l_2 3l_3)+h\nu ,$$

and collisional excitation and deexcitation,

$$X^{+(z-1)}(\bar{2}l_1 3l_2 3l_3)+e^-\rightarrow X^{+(z-1)}(3l_3)+e^- ,$$

$$X^{+(z-1)}(\bar{2}l_1 3l_2 3l_3)+e^-\rightarrow X^{+(z-1)}(\bar{2}l_1 3l_2' 3l_3)+e^- ,$$

$$X^{+(z-1)}(\bar{2}l_1 3l_2 3l_3)+e^-\rightarrow X^{+(z-1)}(\bar{2}l_1' 3l_2 3l_3)+e^- .$$

All of these processes are included in our calculation.

To calculate the population kinetics, let N_I = population of the neonlike ground state, N_j = population of the doubly excited states $j=1$–237, N_{F_i} = population of the sodiumlike nonautoionizing states $i=1$–5, and R_{ab} = rate coefficient for transitions from level a to level b; then,

$$\frac{dN_I}{dt}=\sum_k N_k R_{kI}-N_I\sum_k R_{Ik} , \tag{4}$$

$$\frac{dN_j}{dt}=N_I R_{Ij}-N_j\left[R_{jI}+\sum_i R_{jFi}+\sum_k R_{jk}\right]+\sum_k N_k R_{kj} , \tag{5}$$

$$\frac{dN_{F_i}}{dt}=\sum_k N_k R_{kF_i} . \tag{6}$$

We then calculate the populations of the doubly excited states using dynamic relaxation to steady state. We assume the population of the neonlike ground state is constant N_I and that the populations of the sodiumlike nonautoionizing states are zero. Equation (5) is solved for N_j by setting $dN_j/dt=0$ and then iterating on

$$N_j=\frac{N_I\gamma_j^{\mathrm{DI}}+\sum_k N_k R_{kj}}{\gamma_j^A+\gamma_j^R+\gamma_j^C+\sum_k R_{jk}} , \tag{7}$$

where $\gamma_j^{\mathrm{DI}}=R_{Ij}$ is the dielectronic capture rate which is calculated by detailed balance from the Auger rate γ_j^A:

$$\gamma_j^{\mathrm{DI}}(\theta)=\frac{h^3 n_e}{(2\pi m\theta)^{3/2}}\frac{g_j\gamma_j^A}{2g_I}e^{-\Delta E_j/\theta} , \tag{8}$$

where g_j = degeneracy of the doubly excited state j, g_I = degeneracy of the neonlike ground state, E_j = energy of the doubly excited state j, E_I = energy of the neonlike ground state, and $\Delta E_j=E_j-E_I$. The radiative decay rate γ_j^R and the collisional deexcitation rate γ_j^C stabilize dielectronic capture by the $\Delta n=1$ transitions:

$$\gamma_j^R+\gamma_j^C=\sum_{i=1}^{5} R_{jFi} . \tag{9}$$

We define the total destruction rate γ_j^D to be

$$\gamma_j^D=\gamma_j^R+\gamma_j^C+\sum_k R_{jk} , \tag{10}$$

where the last term is due to $\Delta n=0$ transitions. The recombination rate is then calculated by summing the flux of population from the doubly excited states to the sodiumlike nonautoionizing states:

$$\gamma^{\mathrm{DR}}=\sum_{j=1}^{237} N_j(\gamma_j^R+\gamma_j^C) . \tag{11}$$

The dielectronic-recombination-rate coefficient α^{DR} is defined by

$$\alpha^{\mathrm{DR}}=\frac{\gamma^{\mathrm{DR}}}{n_e N_i} . \tag{12}$$

The inclusion of the radiative decay rates for the $\Delta n=0$ transitions increases the rate coefficient by less than 3% for the range of ions we considered.

III. RESULTS

We calculated the dielectronic-recombination-rate coefficient α^{DR} for the neonlike isoelectronic sequence as a function of electron temperature for each of the 17 elements Ar, Fe, Cu, Ge, Kr, Zr, Nb, Mo, Ru, Rh, Ag, Sn, Xe, Nd, Ho, Ta, and W at an electron density $n_e=10^{14}/\mathrm{cm}^3$. At this density, the effect of electron collisions is negligible and can be neglected as we will show later. In Fig. 1 we plot α^{DR} versus θ for six of the elements. In Table I we list the maximum value of the

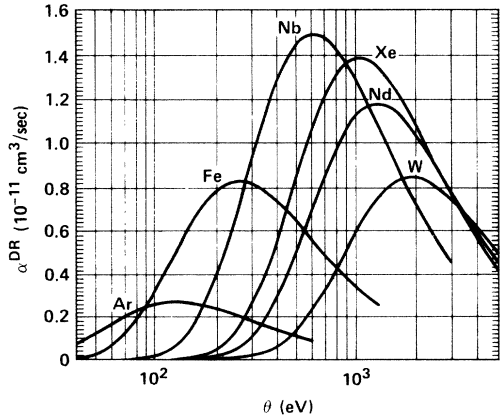

FIG. 1. Dielectronic-recombination-rate coefficient α^{DR} vs electron temperature for six neonlike ions.

TABLE I. Dielectronic-recombination-rate coefficients.

Z	θ_0 (eV)	α^{DR}_{max} (10^{-11} cm^3/sec)	$\bar{E}$ (eV)
18	124	0.265	186.5
26	257	0.825	385.6
29	314	1.109	471.6
32	380	1.235	569.8
36	474	1.382	711.0
40	576	1.489	864.3
41	602	1.495	903.4
42	632	1.488	948.4
44	692	1.470	1037.8
45	724	1.451	1085.3
47	788	1.441	1181.4
50	885	1.423	1326.9
54	1023	1.389	1533.6
60	1257	1.178	1881.4
67	1556	1.009	2327.5
73	1844	0.865	2752.4
74	1881	0.845	2806.5

dielectronic-recombination-rate coefficient α^{DR}_{max} for each element and the value of θ_0 at which α^{DR} is maximum. Also listed is $\bar{E}$, the average energy lost by an electron in each recombination. $\bar{E}$ is calculated by

$$\bar{E}=\frac{\sum_j \Delta E_j\,\omega_j}{\sum_j \omega_j}\ , \tag{13}$$

where

$$\omega_j=\frac{\gamma_j^{DI}\gamma_j^{R}}{\gamma_j^{R}+\gamma_j^{A}}\ . \tag{14}$$

We calculate ω_j at θ_0. The $\sum_j \omega_j$ is a fast numerical algorithm[10] to calculate an approximate γ^{DR}. If we model dielectronic recombination via the $3l3l'$ manifold as proceeding through one pseudo-doubly-excited state with $\Delta E=\bar{E}$, then we may fit the relativistic multiconfiguration rate coefficient by

$$\alpha^{DR}=\frac{4.4817\alpha^{DR}_{max}e^{-3/2x}}{x^{3/2}},\quad x=\frac{3\theta}{2\bar{E}} \tag{15}$$

where α^{DR} is maximum at $\theta=\frac{2}{3}\bar{E}$. (Comparing $\bar{E}$ and θ_0 in Table I, we see that $\theta_0\approx\frac{2}{3}\bar{E}$ within 1% for all elements.) Figure 2 shows α^{DR} plotted versus θ for Nb, demonstrating excellent agreement between the fit and the original data. The circles are a result of the detailed calculation while the solid line represents the fit of Eq. (15). Agreement is better than 1% over the range $0.5<x<5$. In general, this fit is good to 4% over the same range of x for all the ions calculated. At low temperatures, the fit underestimates α^{DR} because the detailed system has lower energy states which become more heavily weighted; therefore, $\bar{E}$ is no longer the appropriate energy to use for the pseudostate.

Figure 3 plots α^{DR}_{max} versus Z (the bare nuclear charge) for this calculation. We note that our calculation for the dielectronic-recombination rate peaks at niobium ($Z=41$).

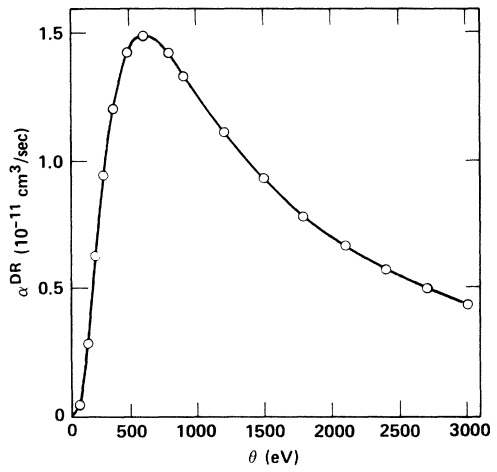

FIG. 2. Dielectronic-recombination-rate coefficient α^{DR} vs electron temperature for neonlike niobium. The circles are the result of this calculation while the solid line is the theoretical fit of Eq. (15).

Collisions can have an effect on α^{DR} by redistributing the population of the doubly excited states among the different angular momentum states of the $3l3l'$ manifold, especially the higher angular momentum states.[11,12] It can also act as a collisional stabilization process by collisionally deexciting a $3l$ state to a $2l$ state. The latter process is very slow, however, except at very high electron densities. In Fig. 4 we plot α^{DR} ($\theta=\theta_0$) versus n_e for four neonlike ions spanning the range of Z we have considered. α^{DR} is normalized to unity for $n_e=10^{14}$. As one might expect, the effect is largest for low Z.

To show the relative effects of angular momentum redistribution ($\Delta n=0$) and collisional deexcitation ($\Delta n=1$) on the net dielectronic-recombination-rate coefficient, we plot in Fig. 5 α^{DR} (at $\theta=\theta_0$) for argon versus

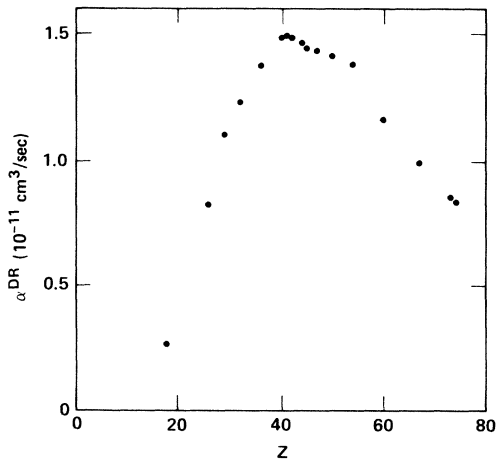

FIG. 3. Maximum value of the dielectronic-recombination-rate coefficient α^{DR} vs the bare nuclear charge Z for 17 neonlike ions.

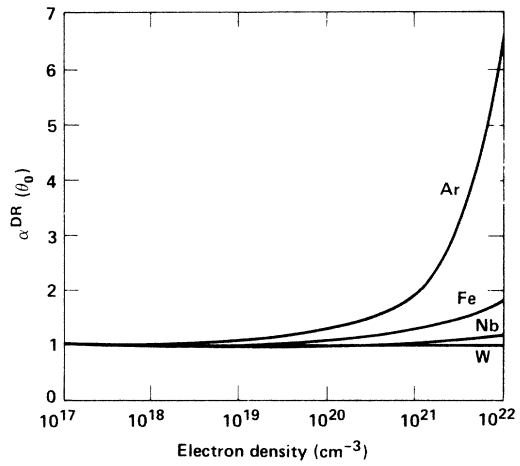

FIG. 4. Dielectronic-recombination-rate coefficient $\alpha^{DR}(\theta_0)$ vs electron density for several neonlike ions. The curves are normalized to unity at $n_e = 10^{14}$.

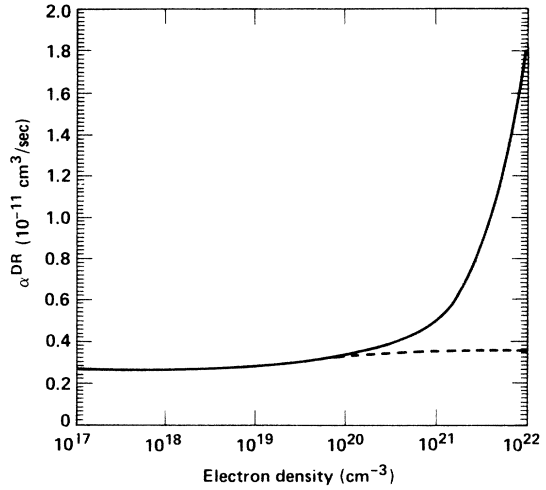

FIG. 5. Dielectronic-recombination-rate coefficient $\alpha^{DR}(\theta_0)$ vs electron density with (solid line) and without (dashed line) electron collisional deexcitation ($\Delta n = 1$) for neonlike argon.

electron density with (solid line) and without (dashed line) collisional deexcitation included in the calculation. Without collisional deexcitation α^{DR} reaches a maximum around $n_e = 10^{21}$ and saturates. This saturation occurs when the collisional rates between the $3l3l'$ states dominate the Auger and radiative rates. The $3l3l'$ states are then in a thermal equilibrium with their relative populations determined by a Boltzmann distribution at the electron temperature. Any further increase in the collision rates ($\Delta n = 0$) will not affect the population distribution since the states are already in local equilibrium. Also, heavy particle collisions[13] can contribute to the angular momentum redistribution especially at high temperatures for very small energy transitions.

As n_e continues to increase, collisional deexcitation ($\Delta n = 1$) becomes dominant over radiative decay in increasing the destruction rate of the doubly excited states. Thus collisions effectively increase the branching ratio for dielectronic capture. As the electron density becomes high enough, this effect will also saturate as the branching ratio reaches unity. It should be pointed out, of course, that at these high values of n_e collisional excitation from the sodiumlike nonautoionizing states (which do have a finite population) will cause a reverse flow and counterbalance the dielectronic recombination.

Finally, the dielectronic-recombination-rate coefficient we have calculated is only a partial rate coefficient. Accurate calculations of the rate coefficient must include principal quantum numbers up to a limit dictated by plasma ionization. We are currently calculating the contributions of the $nln'l'$ manifolds for $n,n' \geq 3$. Convergence of the calculated rates is expected to be fairly rapid for high-Z ions, such as tungsten, for two reasons. First, calculations using the $3l3l'$ manifold for tungsten show that the bulk of the dielectronic-recombination flux proceeds through a reasonably small number of channels. Second, due to j-j coupling, each multiconfiguration wave function used to calculate matrix elements is very pure in one single-configuration wave function for the high-Z ions. In this case, the use of single-configuration wave functions should be a very good approximation, and extension of the dielectronic-recombination-rate coefficient to high-n values can be accomplished quite accurately by semianalytic formulation. Convergence of the low-Z cases, on the other hand, is complicated by the necessity of including virtually all of the $3l3l'$ states to obtain reasonable accuracy. (The results reported here include all states for each calculation.) However, including principal quantum numbers above $n = 4$ will require compromise due to the large number of states for these manifolds. Despite a lower plasma ionization principal quantum number for low-Z ions, computation of converged dielectronic-recombination-rate coefficients for these elements becomes very difficult because of the necessity of retaining virtually every state of the doubly excited manifolds.

ACKNOWLEDGMENTS

The authors would like to thank Rosemary Jung for her invaluable assistance in organizing the computer coding which makes up YODA. The authors would also like to thank L. R. Roszman and S. M. Younger for many useful suggestions. This work was performed under the auspices of the U.S. Department of Energy by the Lawrence Livermore National Laboratory under Contract No. W-7405-ENG-48.

[1]A. Burgess, Astrophys. J. **139**, 776 (1964).
[2]A. L. Merts, R. D. Cowan, and N. H. Magee, Jr., Los Alamos Scientific Laboratory Report No. LA-6220-MS, 1976 (unpublished).
[3]Y. Hahn, J. N. Gau, R. Luddy, and J. A. Retter, J. Quant. Spectrosc. Radiat. Transfer **23**, 65 (1980).
[4]Larry J. Roszman, Phys. Rev. A **20**, 673 (1979).
[5]B. W. Shore, Astrophys, J. **158**, 1205 (1969).

[6]A. Burgess and H. P. Summers, Astrophys. J. **157**, 1007 (1969).
[7]P. J. Mohr, Ann. Phys. (N.Y.) **88**, 26 (1974).
[8]E. A. Uehling, Phys. Rev. **48**, 55 (1935).
[9]A. Burgess, J. Phys. B **7**, L364 (1974).
[10]M. J. Seaton and P. J. Storey, *Atomic Processes and Applications* (North-Holland, Amsterdam, 1976).
[11]V. L. Jacobs and J. Davis, Phys. Rev. A **18**, 697 (1978).
[12]V. L. Jacobs and M. Blaha, Phys. Rev. A **21**, 525 (1980).
[13]J. C. Weisheit, J. Phys. B **8**, 2556 (1975).